

# Utilizing Direct-Push Crosshole Testing to Assess the Effectiveness of Soil Stiffening Caused by Installation of Stone Columns and Rammed Aggregate Piers

L. M. Wotherspoon<sup>1</sup>, B.R. Cox<sup>2</sup>, K.H. Stokoe II<sup>3</sup>, D.J. Ashfield<sup>4</sup> and R.A. Phillips<sup>5</sup>

## ABSTRACT

This paper outlines a methodology for the assessment of the effectiveness of soil stiffening caused by installation of shallow vibro-replacement stone columns (SC) and Rammed Aggregate Piers<sup>TM</sup> (RAP) in Christchurch, New Zealand for liquefaction mitigation. Direct-push crosshole tests were performed before and after ground improvement using custom-built cone sensors to measure compression wave ( $V_p$ ) and shear wave velocity ( $V_s$ ). Full scale case study results presented here and in other studies highlight the usefulness of the crosshole technique, as it can reliably demonstrate the stiffening effect of the composite soil-improvement mass. Crosshole testing showed that the SC and RAP ground improvement techniques seem to develop composite stiffness characteristics of the improved zone through two quite different mechanisms. Vibro-replacement SCs at typically-used area replacement ratios (ARRs) appear to provide greater stiffening of the native clean sand soils within the improved zone compared to the RAP at their typically-used ARR. However, despite less stiffening of the native soil within the improved zone, RAPs appear to be stiffer discrete inclusions than the SCs, as evidenced by their high composite  $V_s$  values, which compensates for the reduced stiffening of the native clean sand soils.

## Introduction

A full-scale field testing program was designed to assess the effectiveness of soil stiffening caused by installation of shallow vibro-replacement stone columns (SC) and Rammed Aggregate Piers<sup>TM</sup> (RAP) for liquefaction mitigation in Christchurch, New Zealand (Tonkin & Taylor Ltd 2014). These ground improvement techniques were installed in soils ranging from clean sands to sandy silts at a number of sites across the city. To assess the stiffening effect, compression wave ( $V_p$ ) and shear wave ( $V_s$ ) velocity measurements were made throughout the depth of the improved zone using direct-push crosshole tests with custom-built cone sensors containing a three-dimensional geophone array. Where possible, tests were performed before ground improvement to characterise the properties of the virgin soil. After ground improvement installation, testing was carried out to characterise the properties of the soil within the improved

---

<sup>1</sup>Research Fellow, Civil & Environmental Engineering, University of Auckland, Auckland, NZ, [l.wotherspoon@auckland.ac.nz](mailto:l.wotherspoon@auckland.ac.nz)

<sup>2</sup>Assistant Professor, Civil, Architectural & Environmental Engineering, University of Texas, Austin, USA, [brcox@utexas.edu](mailto:brcox@utexas.edu)

<sup>3</sup>Professor, Civil, Architectural & Environmental Engineering, University of Texas, Austin, USA, [k.stokoe@utexas.edu](mailto:k.stokoe@utexas.edu)

<sup>4</sup>Tonkin & Taylor Ltd, Christchurch, NZ, [dashfield@tonkin.co.nz](mailto:dashfield@tonkin.co.nz)

<sup>5</sup>Tonkin & Taylor Ltd, Christchurch, NZ, [rphillips@tonkin.co.nz](mailto:rphillips@tonkin.co.nz)

zone (i.e. between SC/RAPs), and the composite properties of the soil and SC/RAP by testing across representative individual SC/RAPs. This paper provides a detailed outline of the direct-push crosshole testing methodology and data interpretation approach used during this study. Results from two case study sites are then presented for stone column and RAP installation in clean sand sites. We focus on the stiffening effect of these ground improvement methods, with small strain shear modulus  $G_{MAX} = V_s^2 \rho$  (where  $\rho$  = density). Other potential beneficial effects of these methods for liquefaction mitigation, such as drainage or increased lateral stress, are not discussed herein.

## **Ground Improvement Methods**

All stone column ground improvements tested as part of this research project were constructed using a dry bottom feed method and river gravel-derived aggregate with at least two broken faces. A vibroflot is first vibrated down to the desired depth of improvement, and then compressed air feeds the stone through the vibratory probe out through its base. As the vibroflot is partially withdrawn, aggregate is delivered into the resulting void and the weight of the vibroflot is applied onto the aggregate in combination with a vibratory load. This process is performed in stages as the probe is progressively withdrawn towards the ground surface to form a column. RAP are also constructed by initially vibrating a mandrel into the soil to the desired depth. The mandrel is partially withdrawn and aggregate is then fed down through the mandrel into the resulting void. Thin layers of aggregate are then compacted using a patented process involving repeated impacts. This process is performed in stages as layers are compacted and the mandrel is withdrawn towards the ground surface to form the RAP. Both methods result in densification of both the aggregate and the surrounding soil.

## **Direct Push Crosshole Testing**

Direct-push crosshole tests were performed to determine  $V_p$  and  $V_s$  as a function of depth using custom-built cone sensors containing a three-dimensional geophone array designed and constructed at the University of Texas. The geophones are housed in a stainless steel cone chassis with dimensions similar to a typical cone penetrometer test (CPT) tip. A source and a receiver sensor were advanced separately into the ground to the same depth using standard CPT rods and two small-scale cone penetrometer rigs. Data was acquired using a Data Physics ACE Quattro dynamic signal analyser connected to a laptop.

The test setup is shown schematically in Figure 1a, with the horizontal spacing between the source and receiver rods ranging from 1.5 – 1.9 m. This distance was defined based on the diameter of the column being tested, using a 500 mm offset on each side of the SC/RAP diameter in an effort to avoid areas of bulging on the side of the SC/RAP that would hinder advancement of the rods. At each test location the sensors were initially pushed to a depth of 0.4 m below ground level and the first test performed. The sensors were then both advanced at 200 mm intervals to determine  $V_p$  and  $V_s$  down to at least 1 m below the depth of SC/RAP installation. CPT operators continually monitored the rods to maintain their verticality during testing.

At each depth testing was performed using a hammer impact source applied to the top of the source rod, with three separate tests performed at each depth and stacked to increase signal-to-

noise ratio. This impact develops compression waves (P-waves) that travel down the length of the source rod to its cone tip. The vertically oriented sensor (SV) at the bottom of the source rod (Figure 1a) was used to trigger the data acquisition system, eliminating the need to determine the P-wave travel time from the source impact at the top of the rod to the wave arrival at the cone tip. The P-wave reaches the end of the rod and creates both radially propagating P-waves and horizontally propagating, vertically polarised shear waves ( $S_{hv}$ -waves) at the base of the source that follow the path shown in Figure 1a.  $S_{hv}$ -waves, referred to as simply S-waves hereafter, were detected by the vertically oriented sensor in the receiver rod (RV). In a similar fashion, P-waves were detected by the horizontal geophone in the receiver rod that was oriented in line with the travel path (RH1). The other horizontally aligned geophone (RH2) is not used in these analyses.

Tests were performed across each SC/RAP to characterise the composite properties of the soil and the SC/RAP, and in-between SC/RAPs to characterise the properties of the soil within the improved zone (Figure 1b). In-between tests were positioned in order to characterise the soil that was furthest away from the SC/RAP elements, representing the soil in the improved zone that was likely to be least affected by the installation of these elements (i.e. the least improved soil). Where possible, tests were performed prior to ground improvement or outside the improved zone to characterise the virgin (or unimproved) soil properties. Similar spacing between source and receiver rods were used for the composite, improved soil zone and virgin measurements at each test location.

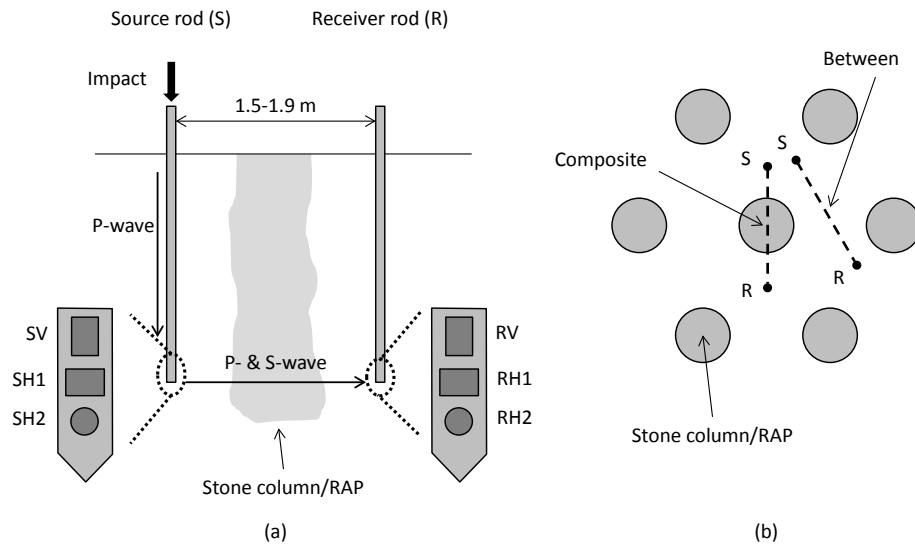


Figure 1: Schematic of the direct push crosshole testing method a) elevation view, b) plan view.

### Calibration method

Throughout the field testing programme, calibration testing was carried out to correct for the trigger calibration time between the source and receiver rods. The source and receiver rods were tightly clamped together above ground using hose clamps at the top and the bottom of the rod. The RH1 and SH1 geophones in the source and receiver rods were aligned, representing the alignment during field testing with a zero separation distance. A hammer impact was applied to the top of the source rod and the waveform recorded with the same data acquisition parameters

used in field testing. Compressive wave (RH1) and shear wave (RV) geophone readings were used to define the trigger calibration time ( $t_T$ ) for each sensor orientation. Typically, the calibration time was negative, meaning that by the time the data acquisition was triggered the vibration had already been detected by the receiver geophones. This type of calibration is important when utilizing source-to-receiver crosshole rather than receiver-to-receiver crosshole.

### *Data interpretation*

The stacked/averaged waveform was used to identify the travel time ( $t_{RAW}$ ) for first arrivals of direct compressive and shear waves at each depth. Waterfall plots that combine traces from each depth into a single plot were used to more easily identify trends with depth, as indicated for the example data in Figure 2. The picked/interpreted direct P-wave first arrivals are shown in Figure 2a, while Figure 2b shows both the picked first arrivals of the direct P-wave from Figure 2a (crosses) and the picked direct S-waves (circles). Once the first arrivals of the direct waves were picked, the velocity ( $V$ ) of each wave type was simply defined using:

$$V = S_R / t_C \quad t_C = t_{RAW} + t_T \quad (1)$$

where  $t_C$  is the corrected travel time and  $S_R$  is the spacing between source and receiver rods.

Picking of the first P-wave arrivals were fairly straightforward, with the first clear departure/break used at each depth. Once saturated soils were encountered, the P-wave arrivals were characterised by a high frequency signal, which is evident in Figure 2a below a depth of 3 m. The main issue to account for in the choice of first arrivals was the effect of P-wave refraction along the saturation depth or other stiff layers. However, refraction effects were minor due to the combination of the short travel distance and small depth increments.

Picking of S-wave first arrivals was complicated by a number of factors, and the first pulse in each trace of the waterfall plots was not always representative of the direct horizontal S-wave travel path. Typically the highest amplitude pulse with the correct polarity (in this case, a positive break/departure) in the initial stages of each trace was assessed as the most likely direct wave arrival. The main sources of waves arriving prior to the direct horizontal S-wave were the result of: (1) A strong P-wave signal arriving near the time of the S-wave may be picked up by the S-wave sensor (RV), which usually only occurred in unsaturated soils where the P-wave velocity was rather slow. This effect is clearly shown in the upper 1.6 m in Figure 2b, with small amplitude signals that start at the point of the P-wave pick at the corresponding depth; (2) If the test depth was near the boundary of a layer with a higher velocity, refracted waves may travel along the layer boundary and arrive at the receiver prior to the direct wave. Usually in this case the amplitude of the refracted wave is less than the direct wave. This effect was often evident below the base of the improved zone, with the amplitude of this refracted wave reducing with depth below this zone. An example of this is shown in Figure 2b below a depth of 5.8 m. Here the stronger amplitude pulse is chosen rather than the smaller amplitude earlier arrivals.

One of the main shortcomings of the receivers used in these trial tests was the inability to measure the subsurface deviation of the source and receiver rods during testing. As stated above, precautions were taken to assure the CPT rods were initially vertical and deviated as little as

possible in the soft soils during testing. Furthermore, the total pushing depths were typically less than 8 m, limiting the distance the rods could drift/deflect over. However, on occasion trends in the  $V_p$  and  $V_s$  with depth were used to identify and account for any deviation issues. Newer versions of the sensors, developed after the conclusion of this testing, have inclinometers installed adjacent to the geophones to allow tracking of the location of the tip of each rod.

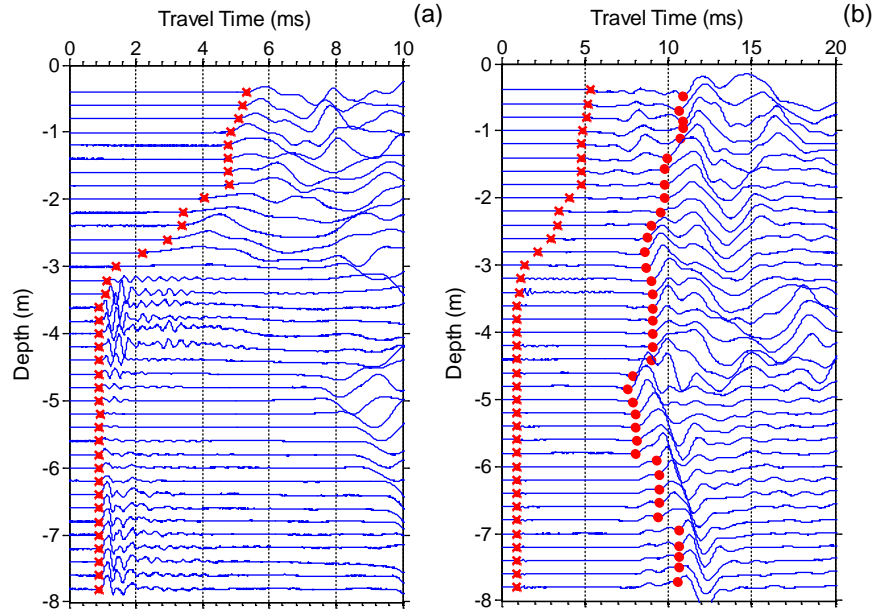


Figure 2: Waterfall plot a) In-line horizontal geophone records used to define compression wave velocity with P-wave picks (crosses); b) Vertical geophone records used to define shear wave velocity with S-wave picks (circles) and P-wave picks from a) (crosses). This waterfall plot is not related to the results presented in Figure 3 or 4.

### Case Studies

The details of two case studies that are presented in this paper are outlined in Table 1. A stone column and a RAP installation are presented, both in predominantly clean sands. The nominal diameter of the SC/RAP, the design spacing, pattern and installation depth, and the average area replacement ratio (ARR, equal to the ratio of the SC/RAP cross sectional area and the improved area) is summarised for each site. Note that the SCs were installed with ARR values approximately twice that used at the RAP sites, with these ARR values fairly representative of recent installations in clean sands in Christchurch. For each case study composite tests are denoted as C, between tests as B, and virgin soil tests as V, with the number of each test also indicated (i.e. C1 for composite test 1).

Table 1: Summary of case study ground improvement details.

Site	Method	Soils	Diameter	Spacing	Depth	ARR	Pattern
A	SC	Clean sand	0.68 m	1.70 m c/c	4.0 m	15.1%	Triangle
C	RAP	Clean sand	0.60 m	2.00 m c/c	4.0 m	8.5%	Triangle

### Stone columns

Figure 3 summarises the soil profile data from crosshole ( $V_p$  and  $V_s$ ) and pre-improvement CPT testing (tip resistance  $q_c$  and soil behaviour type index  $I_c$  (Robertson & Wride 1998)) at Site A, with fines content (FC, % passing 0.075  $\mu\text{m}$  sieve) from laboratory testing of 1-4% in the relatively clean sand profile. The horizontal spacing between source and receiver was approximately 1.7 m at this location, therefore for composite tests, approximately 40% of the travel path was through the SCs.

There is a clear increase in  $V_s$  within and below the column installation depth for all tests (both across/composite C and between B) compared to the virgin soil measurements. Surprisingly, there is little difference in the C (composite) and B (between)  $V_s$  measurements, suggesting that the stiffness of the stone columns elements are not too dissimilar from the stiffness of the surrounding improved soil. Overall, the SC installation increased  $V_s$  by approximately 50 m/s throughout the improved zone, a 70-100% increase in  $G_{MAX}$ . The  $V_p$  measurements are dominated by the degree of soil saturation, and indicate a slight reduction in post-improvement saturation over most of the improved zone. This reduction in the degree of saturation was a characteristic evident at a number of other sites where SCs were installed (Tonkin & Taylor 2014). At Site A testing was carried out 18 days after SC installation.

Pre- and post-improvement CPT soundings were also able to assess the level of improvement of the soil between the SCs across a range of soil types (Tonkin & Taylor Ltd 2014). However, CPT soundings cannot be used to infer the composite soil-column stiffness.

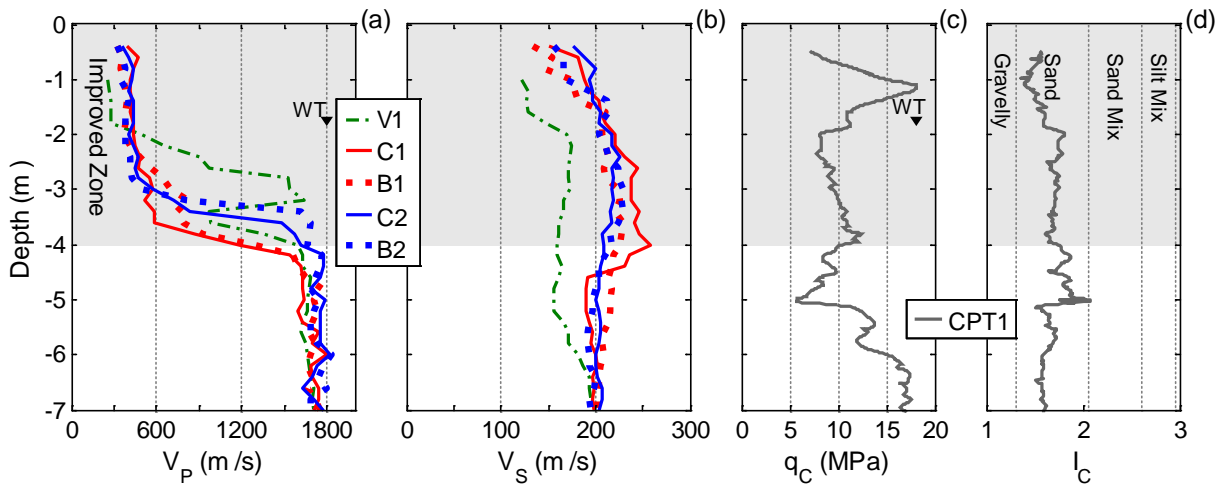


Figure 3: Site A characteristics: a) P-wave velocity; b) S-wave velocity; c) CPT tip resistance; d) soil behaviour type index.

### Rammed aggregate piers

Figure 4 summarises the soil profile data from crosshole and pre-improvement CPT testing at Site B, with fines content from laboratory testing of <5% in the relatively clean sand profile below 1 m depth. The horizontal spacing between source and receiver was approximately 1.6 m

at this location, therefore for composite tests approximately 38% of the travel path was through the RAPs (comparable to the 40% travel path for the SC test summarised here).

Below 1 m depth, the profile is relatively clean sand, and there is a clear difference in the C and B  $V_s$  measurements. Soil between the RAP units showed  $V_s$  increases of approximately 20 m/s compared to the virgin soil measurements throughout the clean sand, an increase in  $G_{MAX}$  of 25-35%. Across the RAP there was a much larger increase in  $V_s$  of between 40-115 m/s in the clean sand, a 180-220% increase in  $G_{MAX}$ . This suggests very effective stiffening of the aggregate in the RAP, and modest stiffening of the soil between RAPs. Consistent with the SC results, there was also an increase in  $V_s$  beneath the improved zone, with this improvement shown to decrease with depth. In this case, the  $V_p$  measurements do not indicate much of a change in the degree of soil saturation in the improved zone before and after installation, a characteristic that was evident at other sites where RAP were installed (Wissman et al. 2015).

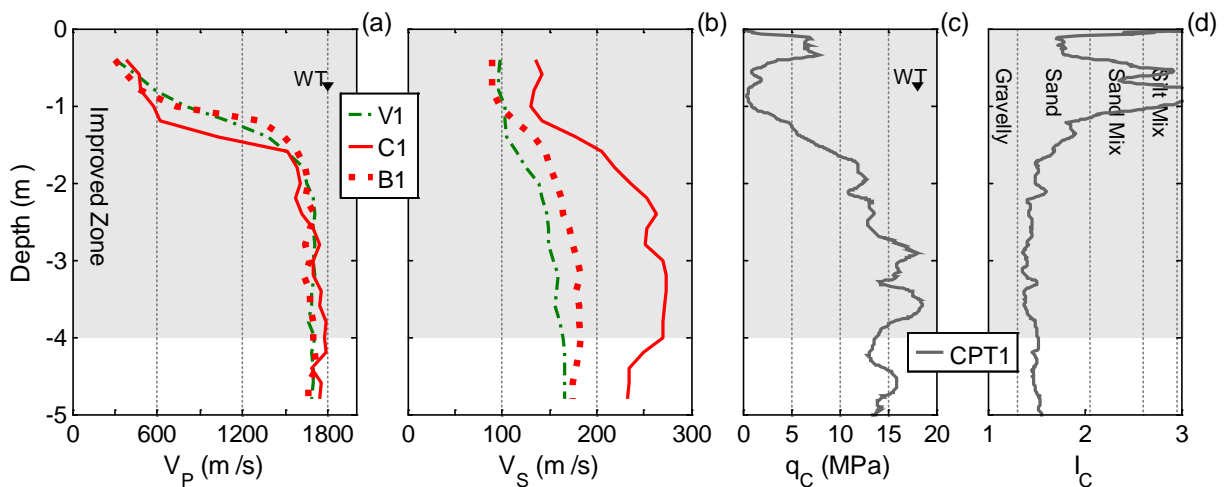


Figure 4: Site B characteristics: a) P-wave velocity; b) S-wave velocity; c) CPT tip resistance; d) soil behaviour type index.

### Verification Testing and Quality Assurance

This and other studies have shown that generally, both vibro-replacement stone columns and RAPs are effective at increasing the  $V_s$  of cleaner sand sites, with the stiffening effect of stone columns and RAPs reducing as the silt content of the soil profile increased (Tonkin & Taylor Ltd 2014, van Ballegooy et al. 2015, Wissman et al. 2015). RAP have been found to be effective in silty sand deposits, however at these sites a high degree of quality assurance (QA) and verification testing was undertaken. In order to ensure that the desired ground improvement characteristics are achieved, verification testing is important when using SC/RAPs, especially in silty soils, so that modifications to the methodology can be made (such as increasing the area replacement ratio) when the desired results are not achieved. While the crosshole method is useful for SC assessment, the improvement of a SC site may be largely demonstrated by CPT soundings in the soil between the columns, as this method seems to rely on an increase in the stiffness of the soil surrounding the SC to provide the desired composite stiffness of the improved zone. Given there appears to be smaller changes in the properties of the soil

surrounding the RAP, crosshole testing may be very useful, as it can reliably demonstrate the stiffening effect of the composite soil-RAP mass.

## Conclusions

This paper outlines the use of direct push crosshole testing to assess the effectiveness of soil stiffening caused by installation of shallow vibro-replacement stone columns (SC) and Rammed Aggregate Piers<sup>TM</sup> (RAP) in Christchurch for liquefaction mitigation. Case study results highlighted the usefulness of the crosshole technique, as it can reliably demonstrate the stiffening effect of the composite soil-improvement mass. More traditional post-construction verification testing methods cannot be used to infer this composite stiffness. Crosshole testing showed that the SC and RAP ground improvement techniques seem to develop composite stiffness characteristics of the improved zone through two quite different mechanisms. Very similar composite (i.e., across columns/RAPs) and between columns/RAPs  $V_s$  measurements were evident at the SC sites, while there was a clear distinction between these measurements at the RAP sites. Thus, the vibro-replacement stone columns at typically installed ARRAs appear to provide greater stiffening of the native clean sand soil within the improved zone compared to the RAP. However, it should be noted that the SCs were installed with ARRAs approximately twice that used at the RAP sites. Despite showing less stiffening of the native soil within the improved zone, RAPs with typically installed ARRAs appear to be stiffer discrete inclusions than the SCs due to their high composite  $V_s$  values, which may compensate for the reduced effect of the RAP on stiffening of the native clean sand soils. A lowering of  $V_p$  was also identified at some SC sites after installation, indicating reductions to the degree of saturation, an effect not evident at RAP installation locations. This change in the degree of saturation over time will be of interest for future study, as it may have an impact on the triggering of liquefaction.

## Acknowledgments

We acknowledge the Canterbury Geotechnical Database for some of the site investigation data used in this study. EQC, CERA, their data suppliers and their engineers, Tonkin & Taylor, have no liability to any user of this data or for the consequences of any person relying on them in any way. This work was partially supported by U.S. National Science Foundation (NSF) grant CMMI-1343524. However, all findings and recommendations expressed in this paper are those of the authors and do not necessarily reflect the views of NSF.

## References

- Robertson PK & Wride CE (1998). Evaluating cyclic liquefaction potential using the cone penetration test, *Canadian Geotechnical Journal* **35**: 442-459.
- Tonkin & Taylor Ltd (2014). *Crosshole seismic testing of stone column ground improvement works*, Factual Report, Tonkin & Taylor Ltd.
- Wissman KJ, van Ballegooy, S, Metcalfe, BC, Dismuke JN & Anderson CK (2015). Rammed aggregate pier ground improvement as a liquefaction mitigation method in sandy and silty soils, *6<sup>th</sup> International Conference on Earthquake Geotechnical Engineering*, 1-4 November, Christchurch, NZ.
- van Ballegooy S, Roberts JN, Stokoe II KH, Cox BR, Wentz FJ & Hwang S (2015). Large-scale testing of shallow ground improvements using controlled staged-loading with T-Rex, *6<sup>th</sup> International Conference on Earthquake Geotechnical Engineering*, 1-4 November, Christchurch, NZ.